Testing and Anchor System Performance of RC Shear Walls Repaired and Strengthened with Externally-Bonded FRP Sheets

C.A. Cruz-Noguez, D.T. Lau & E. Sherwood
Department of Civil and Environmental Engineering, Carleton University, Ottawa

15 WCEE
LISBOA 2012

SUMMARY:
This paper presents the experimental results and preliminary analytical findings of a comprehensive study of reinforced-concrete (RC) shear walls repaired and strengthened using externally-bonded fibre-reinforced polymer (FRP) tow sheets. An innovative anchoring system to transfer the loads carried by the FRP sheets to the foundation of the wall is used. The efficiency of the FRP system to increase the flexural strength and stiffness of slender shear walls designed according to current codes of construction and to enhance the shear strength of squat shear wall specimens representative of deficient, old RC structures, is investigated. Results show that the FRP system significantly improves the flexural strength and stiffness for walls in both repair and strengthening applications. Computer simulations confirm that the FRP system is also effective in eliminating the brittle shear mode of failure in walls with insufficient shear reinforcement and non-ductile details.

Keywords: concrete; FRP; repair; shear wall; test
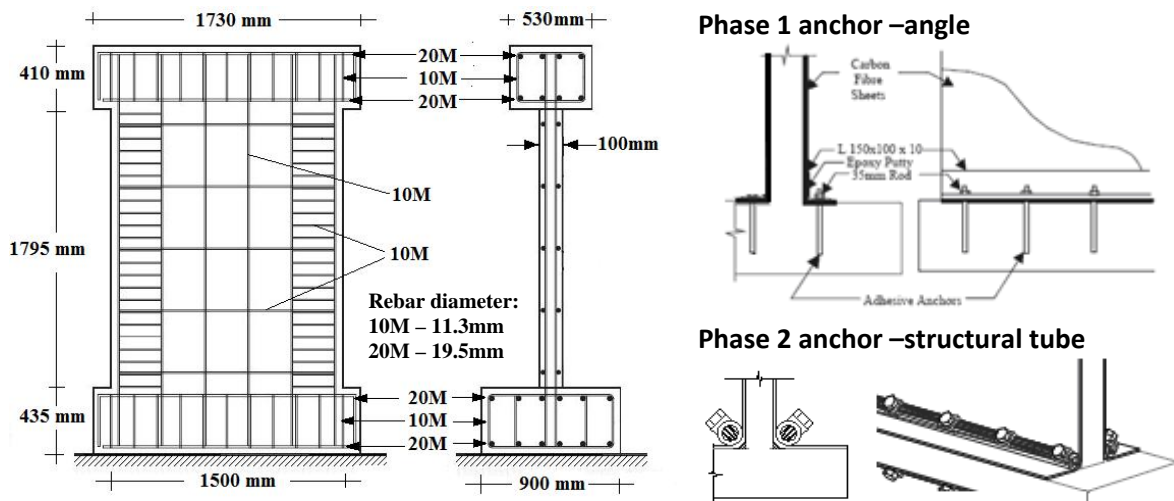
1. INTRODUCTION

Reinforced concrete (RC) shear walls are a common type of lateral load resisting system often found in structures located in seismically active regions. Although current design procedures for shear walls have been significantly improved in recent decades (ACI 318-05; CSA A23.3-04), many older shear wall buildings are at risk of suffering severe damage during moderate or large earthquakes because of insufficient in-plane stiffness, flexural and shear strengths and/or ductility (Lombard et al. 2000). An attractive, minimally-disruptive option for the repair and strengthening of shear walls in existing RC structures is the use of fibre-reinforced polymers (FRP) sheets (Triantafillou 1998). The use of FRP materials to repair and retrofit structural elements in existing buildings has increased in recent years due to the ease in installation, high strength-to-weight ratio, and high resistance to corrosion that FRP materials offer (Meier et al. 1992). Most of the research conducted on FRP-reinforced shear walls has been aimed at increasing the shear strength and energy dissipation capacity of walls with insufficient shear reinforcement and non-ductile details (Antoniades et al. 2003; Paterson and Mitchell 2003; Khalil and Ghobarah 2005). In contrast, the number of studies that address the use of FRP to increase or recover the flexural strength of RC shear walls is limited (Lombard et al. 2000; Hiotakis 2004) due to the possibility of facilitating a brittle shear failure in the walls. However, in situations where increasing the flexural strength of shear walls is unavoidable (i.e., in old structures where the demands calculated according to modern provisions exceed the provided strength), the use of flexural FRP reinforcement may be justifiable. For flexural FRP strengthening/repair applications to be effective, the increment in flexural strength must be accompanied by an appropriate improvement to shear strength capacity of the wall, in order to ensure the avoidance of the brittle shear failure mode. A reinforcing scheme for RC shear walls, consisting of externally-bonded carbon FRP (CFRP) sheets is discussed in this paper. The study has been divided in three phases. The objectives in Phases 1 and 2 were to investigate the effectiveness of the FRP system in recovering or improving the flexural strength and stiffness of shear walls designed according to current code provisions (CSA, 2004), while maintaining a ductile response, while walls with insufficient shear reinforcement and non-ductile

details (lap splices at the plastic hinge region of the walls and edge zones without adequate confinement) are addressed in Phase 3 of the study, currently underway at Carleton University. The experimental results obtained in Phases 1 and 2 in terms of failure mechanisms, stiffness and load capacity are discussed. The design methodology and preliminary analytical results from Phase 3 are also presented.

2. EXPERIMENTAL PROGRAM (PHASES 1 AND 2)

2.1. Design Methodology

The effectiveness of CFRP reinforcement oriented in the vertical direction for repair and strengthening of RC shear walls in flexure has been evaluated by Lombard et al. (2000) and Hiotakis (2004) through the testing of nine cantilevered 1.8x1.5x0.1 m shear wall specimens (Fig. 1) subjected to cyclic lateral loading applied at the top of the wall. All walls are designed according to the CSA A23.3 (2004) specifications in their un-repaired/ un-strengthened state to ensure that they exhibit a ductile failure before the calculated shear strength is reached. The longitudinal and transverse reinforcement ratios of the wall specimens are 0.8 and 0.5%, respectively. The height-to-length ratio of the walls is 1.20.

Figure 2.1 Shear wall details, Phases 1 and 2 (Lombard et al. 1999; Hiotakis, 2004)

Table 1.1. Repair/Strengthening Schemes

Phase	Anchor type	Type of Specimen	Repair/Strengthening Scheme*	Code
1	Angle	Control	---	CW-1
		Repaired	1V	RW-1
		Strengthened	1V	SW1-1
		Strengthened	2V + 1H	SW2-1
2	Tube	Control	---	CW-2
		Repaired	1V	RW-2
		Strengthened	1V	SW1-2
		Strengthened	2V	SW2-2
		Strengthened	3V + 1H	SW3-2

*: nV = Wall reinforced with n layers of unidirectional FRP on each side in the vertical direction
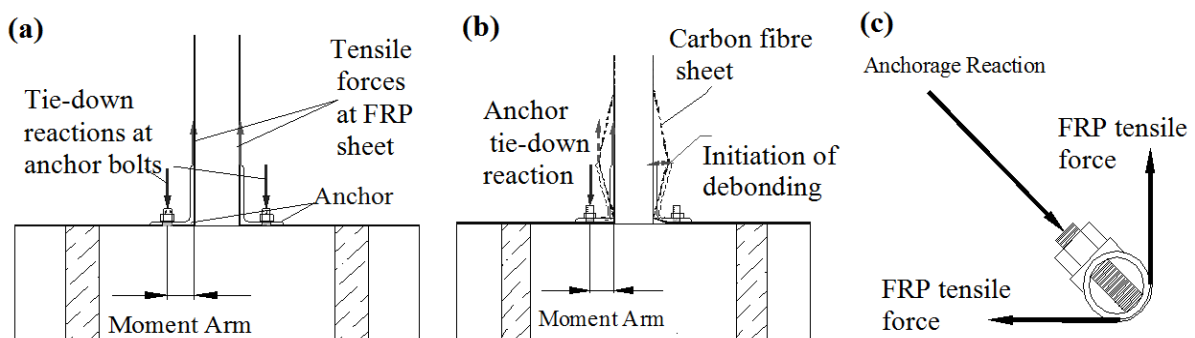*: mH = Wall reinforced with m layers of unidirectional FRP on each side in the horizontal direction

Two different anchoring systems were used to transfer the load from the FRP sheets to the foundation in Phases 1 and 2. In Phase 1, the anchor consists of an off-the-shelf structural steel angle, while an innovative structural tube anchor system is used in Phase 2 (Table 1). The wall specimens include two repaired walls (RW), five strengthened shear walls (SW) and two control walls (CW). The control walls have no FRP reinforcement and are tested in its original state to serve as a baseline for the evaluation of the repair and strengthening techniques, simulating conventional RC walls that have

suffered damage from a moderate to large earthquake. After the CW specimens are tested, they are repaired (the cracks are filled with mortar and CFRP tow sheets are epoxied to the surface) and designated as RW specimens. In contrast, the SW specimens are previously undamaged walls with CFRP reinforcement schemes identical to those of RW specimens, subjected to the same load protocols. The FRP repair/strengthening system was designed in all cases to increase the flexural strength while avoiding a brittle shear failure (Lombard et al. 2000). Details on the FRP-reinforcing scheme used for each specimen are shown in Table 1.
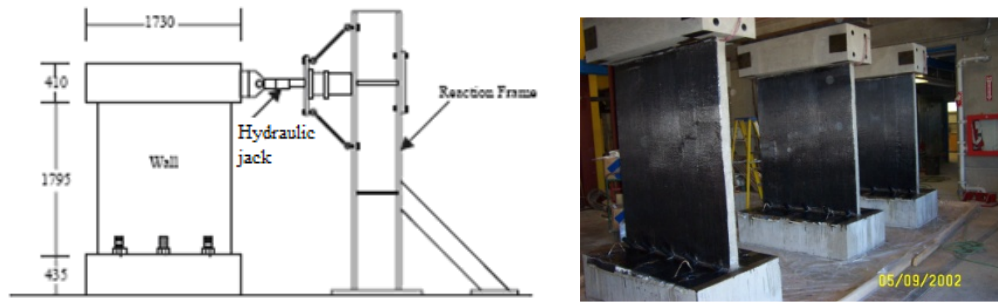
2.2. Anchoring systems

Since the vertically-oriented sheets had to be anchored to efficiently transfer the load from the sheets to the foundation, the anchoring system is critical for the success of this retrofit technique. The anchoring system in Phase 1 consisted of an L150x100x10, 400 MPa structural steel angle bonded to the vertical carbon fibre sheets with epoxy putty (Fig. 2.2[a]). This anchoring method was selected because structural angles are relatively inexpensive and they can be readily manufactured in a wide range of dimensions and sizes. Experimental observations in Phase 1 of the study showed that under force levels higher than the load associated to yielding of the longitudinal reinforcement, the vertical flange of the L-shaped angle of separated from the wall, leading to premature debonding of the CFRP sheet from the concrete substrate and rupture of the FRP material (Fig. 2.2[b]). This rotation in the angle (also referred as "prying" action) was caused by a rotation of the angle, induced by the moment arm between the tensile force carried by the CFRP sheet and the tie-down reaction of the anchoring bolts. In Phase 2 of the study, an innovative tube anchor was designed to eliminate the rotation observed in the L-shaped angle of Phase 1. The new anchor is designed based on the pulley principle using a cylindrical hollow section (Hiotakis, 2004). By wrapping the CFRP sheet around the tube (Fig. 2.2[c]), the anchor acts as pulley and the vertical tensile force carried by the CFRP sheet equates the tensile force developed at the interface between the horizontal segment of the sheet and the concrete surface of the footing. The tube is anchored on the wall footing by threaded anchor bolts installed at a 45-degree angle in the direction of the resultant of the two forces developed on the wall and the footing, which eliminates any eccentricity in the forces acting on the anchor. An optimization study of the innovative tube anchor to provide a reduction in size and simplify its design using finite-element simulations is discussed in Section 3 of this paper.

Figure 2.2 a) Forces acting on the angle anchor; b) prying action; c) forces acting on the tube anchor (Lombard et al. 1999; Hiotakis, 2004)
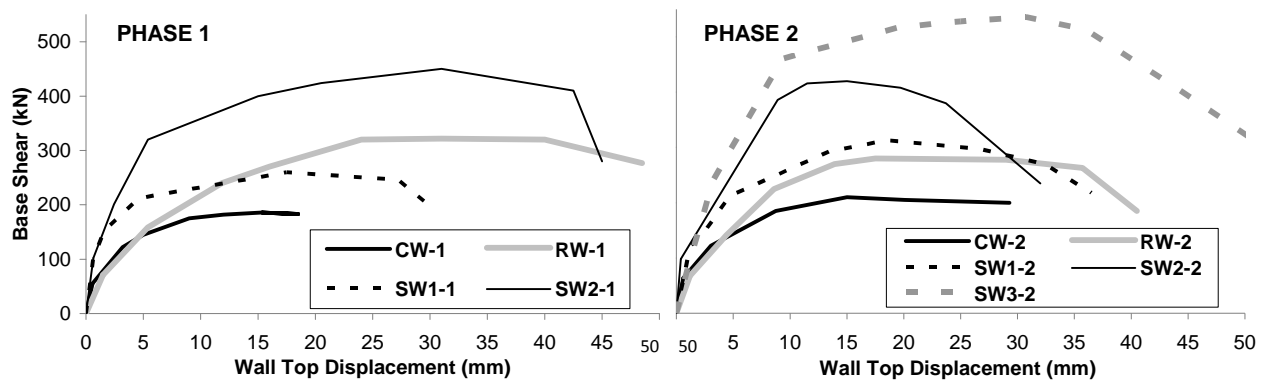
2.3. Experimental Setup

All specimens were tested first under a predetermined in-plane quasi-static cyclic loading sequence in load control up to the yield load, and then continuing in displacement-controlled cycles reaching predetermined displacement ductilities up to failure. The specimens were fixed at the base with threaded rods to the laboratory's strong floor. The lateral load is applied at the top of the specimen through a horizontal cap beam by a hydraulic actuator supported by a reaction frame. The walls were tested in single curvature. The out-of-plane deformation of the shear wall is restrained in the tests of Phase 2. The test set-up and wall specimens are shown in Fig. 2.3.

Figure 2.3 Experimental setup (Phases 1 and 2) and wall specimens (Lombard et al. 1999; Hiotakis, 2004)

2.4. Experimental Results

Figure 2.4 Force-displacement envelopes (Phases 1 and 2) measured for slender wall specimens
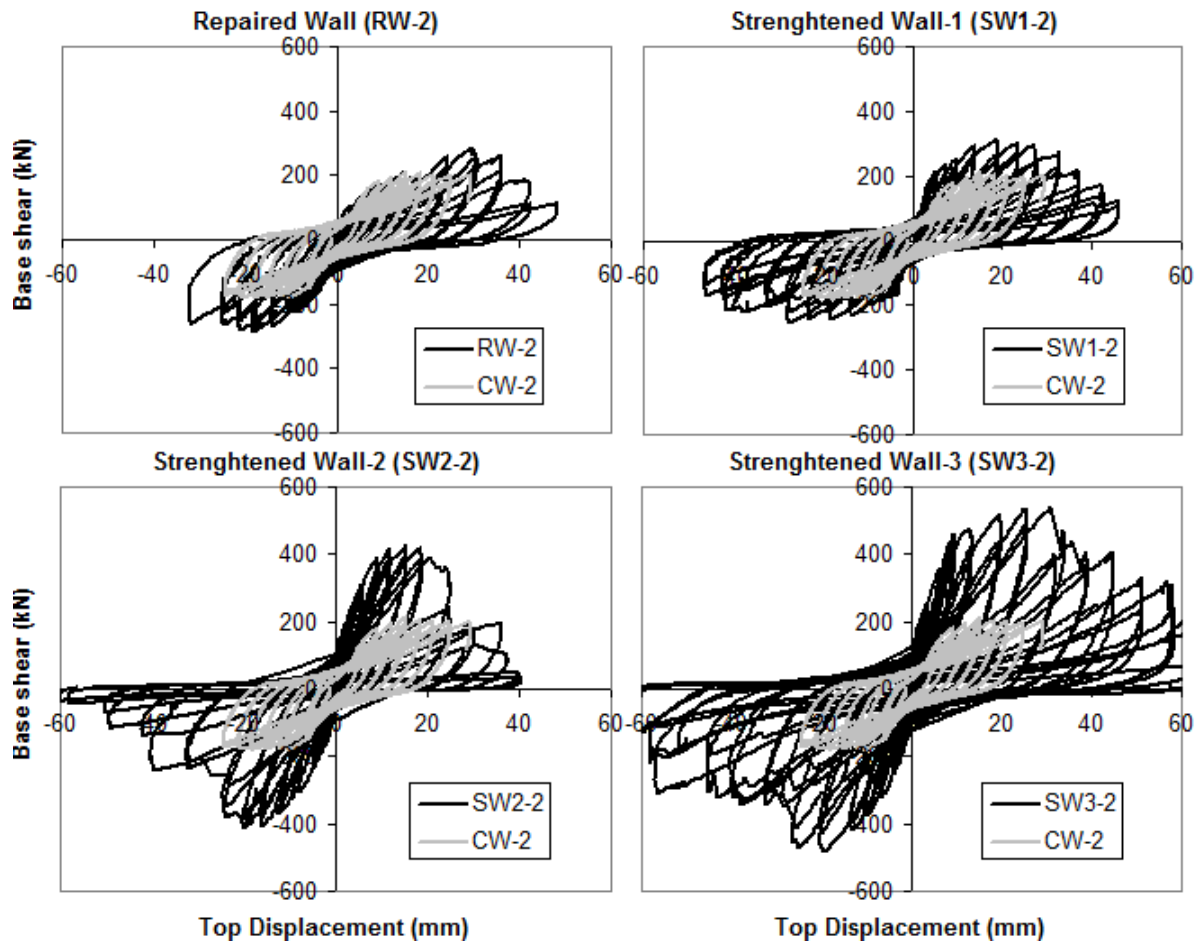
Table 2.1. Measured structural parameters, Phases 1 and 2 (Lombard et al. 1999; Hiotakis, 2004)

EXPERIMENTAL RESPONSE	SPECIMEN								
	CW-1	RW-1	SW1-1	SW2-1	CW-2	RW-2	SW1-2	SW2-2	SW3-2
Cracking Load (kN)	55.1	71.1	101.1	102.0	63.5	67.8	120.1	98.3	146.7
Cracking Displacement (mm)	0.57	1.48	0.64	0.64	0.53	1.19	1.20	0.40	0.98
Cracking Secant Stiffness (kN/mm)	96.6	47.9	158.7	159.9	122.7	57.0	101.4	295.6	149.7
Cracking Stiffness compared to CW (ratio)	1.0	0.5	1.6	1.7	1.0	0.5	0.9	2.6	1.2
Yield Load (kN)	122.4	158.4	152.1	201.2	122.3	140.8	151.7	204.9	240.9
Yield Load Displacement (mm)	3.74	5.39	1.59	2.43	3.04	4.37	2.68	3.55	3.25
Yield Load compared to CW (ratio)	1.0	1.29	1.24	1.64	1.0	1.2	1.2	1.7	2.0
Yield Secant Stiffness (kN/mm)	32.8	29.4	95.5	82.8	40.2	33.2	57.6	59.1	74.2
Yield Stiffness compared to CW (ratio)	1.0	0.9	3.0	2.5	1.0	0.8	1.4	1.5	1.8
Maximum Load Carrying Capacity (kN)	177.6	320.7	258.8	413.1	196.5	280.3	313.0	419.4	514.2
Displacement at maximum load (mm)	15.25	31.00	17.50	31.00	12.78	25.40	23.04	17.49	25.05
Increase in Load Carrying Capacity (ratio)	1.0	1.8	1.5	2.3	1.0	1.4	1.6	2.1	2.6

Fig. 2.4 clearly illustrates the efficiency of the CFRP flexural reinforcing system to restore or increase the load capacity and ductility in both repaired and strengthened walls. In terms of initial stiffness, in strengthened specimens this parameter is significantly increased. In repaired walls, the CFRP system is able to restore most of the initial stiffness.

The results obtained for the control specimens during Phases 1 and 2 show that both walls had similar maximum load carrying capacities (with the maximum load capacity of CW-2 being 9.6% higher than that of CW-1). The only significant difference consisted on the larger displacement demands on CW-2, purposefully applied with the objective of testing the CFRP reinforcement system on a wall with a higher amount of damage compared to CW-1. Once the control walls are repaired, the initial secant
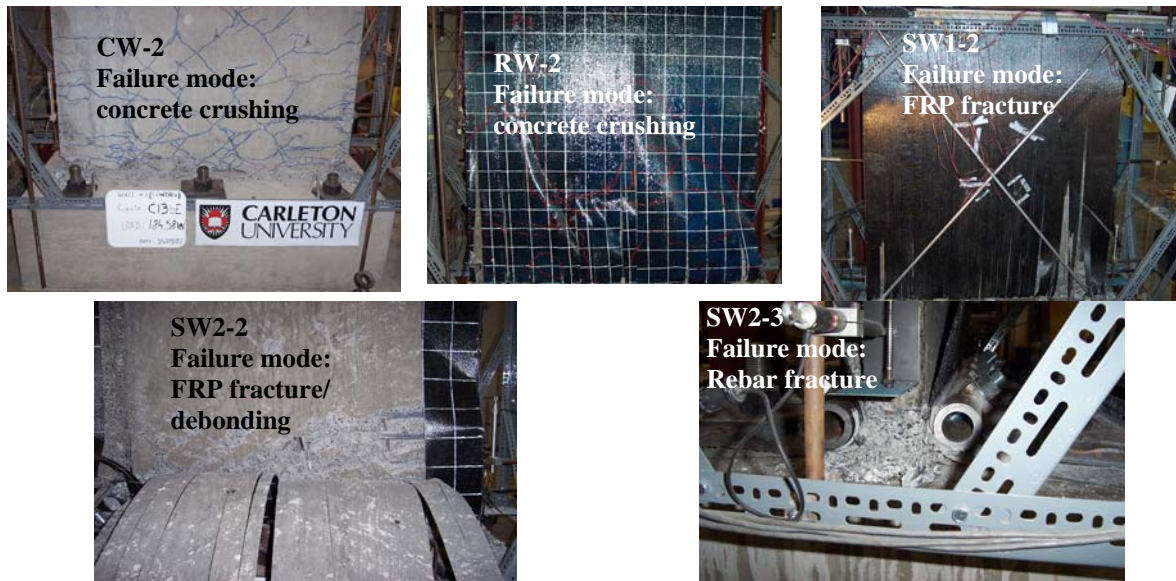
stiffness is mostly recovered (90% in Phase 1 and 80% in Phase 2). Re-opening of cracks before the walls reach their yielding load marks the initiation of FRP debonding. The maximum load carrying capacity is increased by 80% and 40% for Phases 1 and 2, respectively. The observed difference in performance between Phases 1 and 2 is attributed to the fact that the CW-2 specimen was purposefully loaded to a larger displacement level than specimen CW-1 (as discussed above) therefore sustaining more damage. In both RW-1 and RW-2, complete tearing of the FRP material is observed before the wall reaches its maximum load capacity. Failure of both walls occurs due to concrete crushing at the wall toes.

Figure 2.5 Hysteretic base shear-top deflection response measured during Phase 2

For the case of the SW specimens reinforced with a single layer of CFRP (SW1-1 and SW1-2), the initial stiffness of the walls increases by 191% and 43% compared to specimens CW-1 and CW-2, respectively. Despite this difference in stiffness, in both walls approximately the same yielding load is achieved (152.1 kN and 151.7 kN in specimens SW1-1 and SW1-2, respectively). The discrepancy in the amount of initial stiffness observed for these walls can be attributed to differences in construction (i.e., asymmetry in the placing of the longitudinal rebars) that may have had an influence on the flexibility of the wall at small displacement levels. The increase in maximum load capacity in the SW1-1 and SW1-2 specimens is 46% and 59%, respectively. The fact that specimen SW1-2 has a maximum load significantly larger (21%) than SW1-1 was caused by the failure of the anchor system in specimen SW1-1, due to pull-out of the anchoring bolts at a force level of 200 kN. Although the wall is later repaired and the test resumes, this effectively affects its maximum load carrying capacity. Specimen SW1-1 fails due to concrete crushing of the wall toe, with negligible FRP tearing, while specimen SW1-2 fails due to fracture of the FRP at the displacement level corresponding to its maximum load capacity. This is because the failure of the anchoring system in specimen SW1-1 prevents the FRP to fully reach its tensile strength capacity.

Figure 2.6 Final state of wall specimens in Phase 2 (Hiotakis, 2004)

The response of the two specimens reinforced with two vertical layers of FRP (SW2-1 and SW2-2) can not be directly compared due to the additional horizontal layer of CFRP installed in the SW2-1 specimen. The most immediate difference is clearly visible in Fig. 4: specimen SW2-1 exhibits a significantly higher ductility compared to specimen SW2-2 (77% more at the displacement associated to the maximum load capacity). This result agrees with previous research on shear walls repaired and retrofitted with horizontal FRP reinforcement (Khalil and Ghobarah, 2005). The maximum load capacity is increased by 132% and 113% in specimens SW2-1 and SW2-2, respectively, and the initial stiffness is increased by 150 and 50% for the same walls. Failure in both walls occurs due to fracture of the FRP reinforcement. In specimen SW3-2, the initial stiffness is increased by 80% and the increment of the load capacity is 160%. Failure occurred due to fracture of the longitudinal reinforcement.

2.5. Observed debonding progression

In Phases 1 and 2, failure is observed to be a gradual process for both RW and SW specimens. The first sign of damage is cracking of the concrete at the zones of the wall near the base. Debonding of the CFRP sheets from the concrete substrate follows, occurring at the cracked zones of the wall. In repaired walls, the damaged state of the walls promotes the debonding of the CFRP sheets from zones of the wall where pre-existing cracks re-open. In the strengthened specimens where premature debonding due to the "prying" action at the angle anchor is prevented (Phase 2), debonding is first observed at the edges of the wall, at zones where the concrete showed opening of major flexural cracks, a phenomenon referred as intermediate crack (IC) debonding (Lu et al. 2005). After debonding is initiated at the bottom part of the edges of the wall in both RW and SW specimens, it propagates rapidly within a few loading cycles to the center of the wall and progresses upwards from that point. Within a few loading cycles after the onset of debonding, the fibres start to fracture at the wall edges. Rupture of the fibres in areas where the FRP has debonded from the concrete because of the opening of a crack is attributed to the high stresses in the FRP resulting from the incompatibility of strains between FRP and concrete at crack zones. On the other hand, the high nonlinearity in the stress profile at the cross section of the wall (due to yielding of the longitudinal reinforcement) confine most of the tearing of the CFRP sheets at the wall boundaries; only the strip of CFRP material located at the central portion of the wall remains intact and bonded to the concrete.

3. PRELIMINARY ANALYTICAL RESULTS OF PHASE 3

3.1. Analytical study

In this section, the use of externally-bonded CFRP sheets to repair and strengthen eight shear wall specimens with insufficient shear reinforcement (horizontal reinforcement ratios less than 0.25) and non-ductile details (lap splices at the plastic hinge region) is analyzed numerically using finite-element models. These structural details are typically found in buildings designed using old construction codes (ACI, 1968; CSA, 1977). The aspect ratio of the walls, h/l, where h is the height of the wall and l is its length, is another parameter under study. This numerical study is part of an experimental and analytical investigation currently underway at Carleton University, consisting of the testing of eight shear wall specimens with insufficient shear reinforcement. The wall inventory includes two slender walls, $h/l =1.20$ (specimens SL), two squat walls with $h/l =0.85$ (specimens SQ1), two squat walls with $h/l =0.65$ (specimens SQ2), and two SQ2 specimens fabricated with a combination of insufficient shear reinforcement and lap splices at the plastic hinge. The height of all walls is constant, 1.8 m, and the length-to-thickness ratio is equal to 15. In their un-repaired and un-strengthened state, all walls have longitudinal and transverse reinforcement ratios of 3% and 0.25%. This ensures that the walls will exhibit a brittle shear failure before they reach their flexural strength.
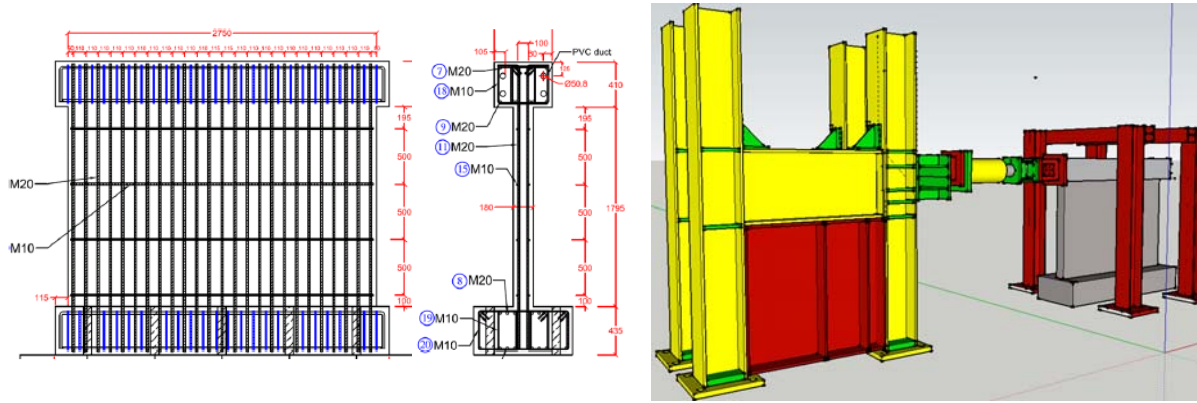

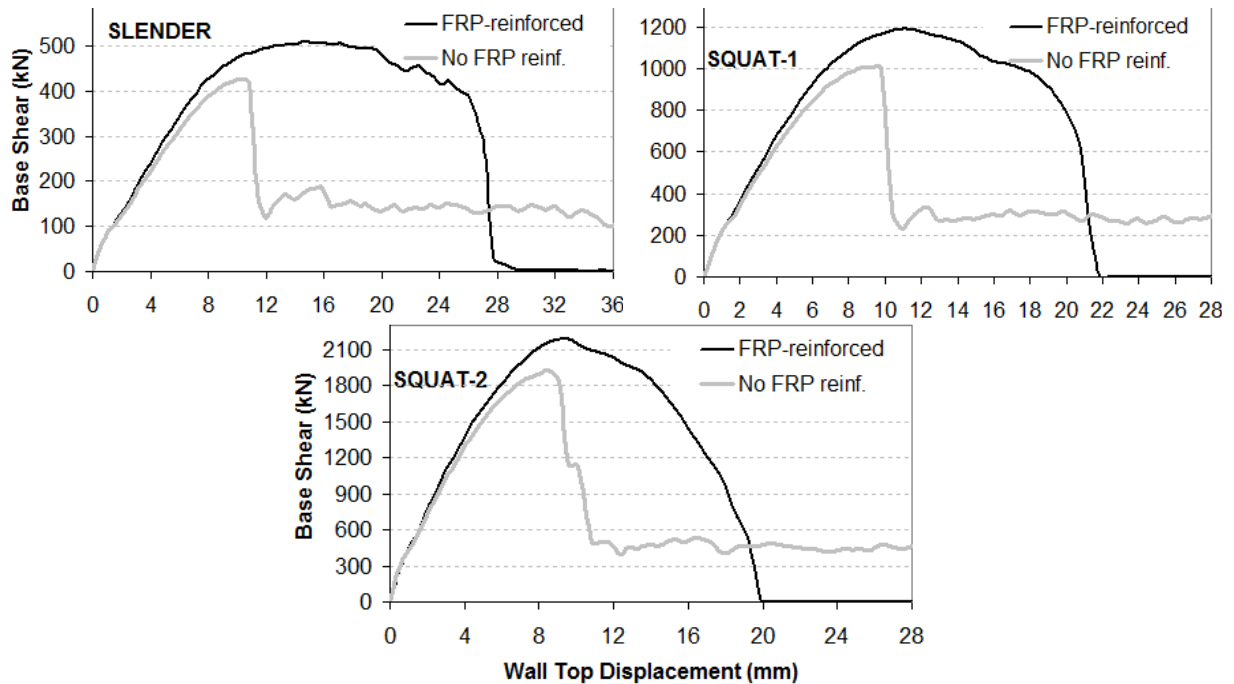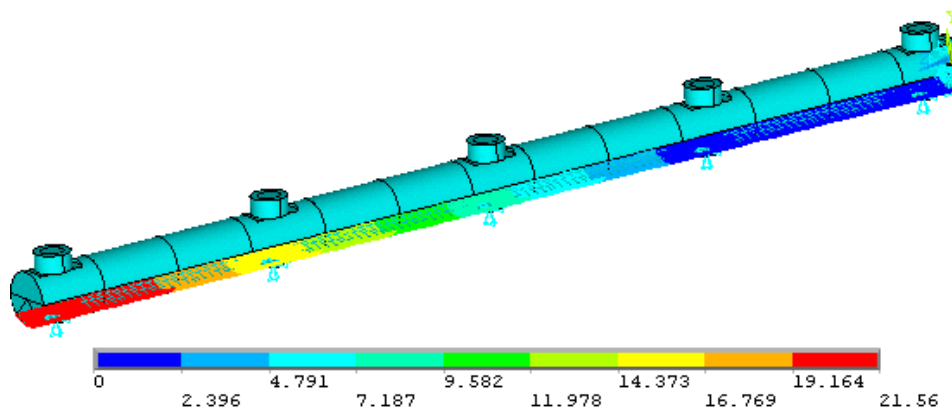**Figure 3.1** Details of specimen SQ2 and experimental setup for Phase 3

Figure 3.2 Force-displacement response for walls with insufficient shear reinforcement in Phase-3

To model the response of the shear walls a finite-element program, VecTor2 (Wong and Vecchio, 2002), was used. Program VecTor2 implements the Modified Compression Field Theory (MCFT) formulated by Vecchio and Collins (1986), and the Disturbed Stress Field Model (DSFM) proposed by Vecchio (2000) for the study of RC concrete subjected to normal and shear stresses. In these formulations, the concrete is modeled as an orthotropic material with smeared, rotating cracks. The CFRP sheets are represented by a series of discrete trusses made of a brittle material with zero compressive strength connected to the concrete through interface link elements. This program has been used successfully to simulate the nonlinear response of shear walls flexurally-reinforced with FRP (Cruz-Noguez et al. 2012). Fig. 3.2 shows the nonlinear response of Squat Wall-2 with and without horizontal FRP reinforcement calculated using VecTor2. A significant improvement in the response can be observed in terms of ductility enhancement for all walls. The ductility increment is higher in specimen SL and comparatively smaller in the squat walls. This is attributed to the fact that the strength of SQ1 and SQ2 walls relies on arch action mechanisms, as in the case of a deep beam, which have limited ductility (MacGregor and Bartlett, 2000) compared to the behaviour dominated more predominantly by flexure (beam action) in specimen SL.
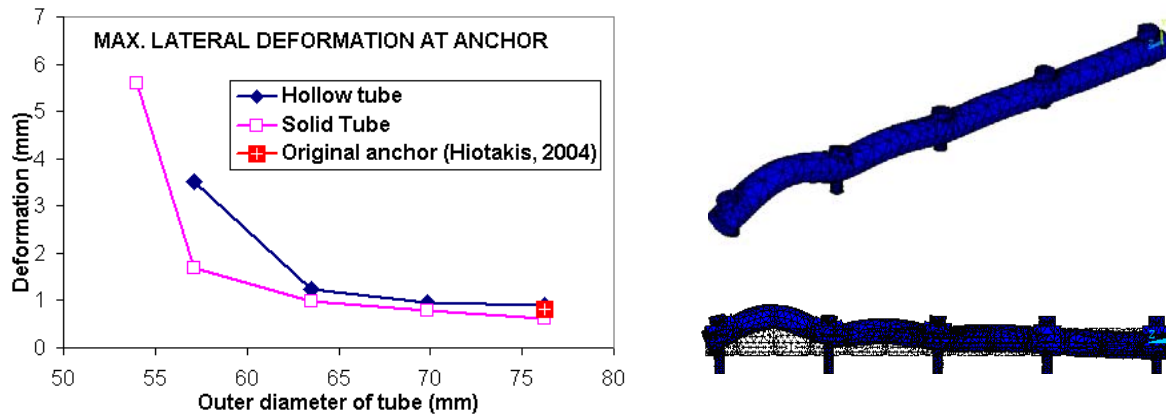
3.2. Tube anchor optimization

The innovative tube anchor used in Phase 2 was shown to prevent the premature debonding of FRP. To reduce the size of the anchor and simplify its constructive details, two different models were developed using the finite-element program ANSYS, with the objective of studying the influence of geometric details on the lateral deformations calculated at the anchor: a) hollow tubes with an outer diameter smaller than that of the tube used in the previous study, 76.2 mm [3 in]; b) solid tubes with diameter smaller than 76.2 mm. The load acting over the tube is considered to be a triangular distributed load, exerted by the portion of FRP in tension (it is assumed that plane section remains plane and the strain distribution in the FRP is linear, varying from a maximum occurring at the tensile fibre to zero at the depth of the neutral axis, as shown in Fig. 3.3). The maximum design load was determined considering the tensile strength of two CFRP sheets. The neutral axis of the wall at the point where the FRP reached its tensile strength was assumed to be located at 35% of the wall length (Hiotakis, 2004). The triangular distributed load was applied to the tube anchor as an equivalent pressure acting on the tube. A plot showing the lateral deformations measured in the tubes for different diameters is shown in Fig. 3.4 (larger displacements translate into loss of load transfer between FRP and concrete). Notice that the diameter of the threaded rods that hold the tube anchor to the foundation is kept constant (31.75 mm [1.25 in]), since the applied loads over the tube anchor are same in all cases, regardless of the size of the tube anchor (the triangular design load remains constant). The analysis was conducted considering a length of tube anchor equal to 1500 mm (specimen SL).

Fig. 3.3 – Pressure load acting at the bottom of the anchor tube (MPa)

Fig. 3.4 – Maximum lateral deformation calculated at anchor (left) and FE model of tube with deformed configuration (right)

Note that in Fig. 3.4 the results for outer diameters larger than 76.2 mm (3.0 in) are not shown since they do not lead to design optimizations, increasing instead the material required for the fabrication of the tube. Only results for outer diameters smaller than 76.2 mm (3.0 in) are presented. Note that yielding occurs at most of the models for diameters smaller than 63.5 mm (2.5 in), regardless of the type of tube used (hollow or solid), with the lateral displacements reaching relatively high values. It is seen that a solid tube can be used with diameters between 57.15-63.5 mm (2.25-2.5 in), optimizing the volume of material by 33-25%. A hollow tube can be used provided the diameter is not taken less than 63.5 mm (2.5 in).

4. CONCLUSIONS

This paper presents the results obtained from a multi-phase study on the repair and strengthening of nine RC shear walls using externally bonded CFRP tow sheets. The conclusions that can be drawn from the study are the following:

a) The carbon fibre repair system can be used to recover the majority of the initial elastic stiffness and to increase the maximum flexural capacity of seismically damaged walls.

b) In strengthening applications, the carbon fibre sheets can be used to significantly increase the stiffness and the ultimate flexural capacity of undamaged walls.

c) The anchoring system is a critical part of the carbon fibre repair/strengthening scheme. The prying action exhibited by the steel angle and the resulting debonding of the sheets prevents the carbon fibre sheets to reach their ultimate tensile strength in RW and SW specimens from Phase 1. The angle and the tube anchor had similar performances in terms of enhancement of initial stiffness and maximum load capacity. However, the angle anchor system was shown to be more prone to premature failures compared to the tube anchor.

d) FRP-debonding caused by the opening up of pre-existing cracks in RW specimens and presence of major flexural cracks in SW specimens is an important factor that largely influences the response of walls flexurally-reinforced with FRP.

e) Numerical simulations showed that a reinforcing scheme based on horizontal CFRP layers can enhance the response of walls with insufficient shear response and non-ductile details by eliminating brittle failure modes due to shear.

REFERENCES

ACI 318. (1968). Building Code Requirements for Structural Concrete. American Concrete Institute, Detroit, Michigan, USA.

Antoniades, K., Salonikios, T., and Kappos, A. (2003). Cyclic Tests on Seismically Damaged Reinforced Concrete Walls Strengthened Using Fiber-Reinforced Polymer Reinforcement. *ACI Structural Journal.* **100:4**, 510-518.

Antoniades, K., Salonikios, T., and Kappos, A. (2005). Test on Seismically Damaged Reinforced Concrete Walls Repaired and Strengthened Using Fiber-Reinforced Polymers. *ACI Structural Journal.* **9:3**, 236-246.

Cruz-Noguez, C., Lau, D. T. and Sherwood, E. (2012). Analytical modeling of reinforced concrete shear walls with externally-bonded CFRP reinforcement. *6th International Conference on Advanced Composite Materials in Bridges and Structures*, ACMBS-VI.

CSA (1977). Code for the Design of Concrete Structures for Buildings. CAN3-A23.3-M77, Canadian Standard Association, Rexdale, Ontario, Canada.

CSA A23.3 (2004). Design of Concrete Structures, Canadian Standards Association, Rexdale, Ontario, Canada.

Hiotakis, S. (2004). Repair and Strengthening of Reinforced Concrete Shear Walls for Earthquake Resistance Using Externally Bonded Carbon Fibre Sheets and a Novel Anchor System. Master's thesis, Department of Civil and Environmental Engineering, Carleton University.

Khalil, A. and Ghobarah, A. (2005). Behaviour of Rehabilitated Structural Walls. *Journal of Earthquake Engineering.* **9:3**, 371-391.

Lombard, J. (1999). Seismic strengthening and repair of reinforced concrete shear walls using externally-bonded carbon fibre tow sheets. Master's thesis, Department of Civil and Environmental Engineering, Carleton University.

Lombard, J., Lau, D., Humar, J., Foo, S. and Cheung, M. (2000). Seismic strengthening and repair of reinforced concrete shear walls", *12th World Conference on Earthquake Eng.* (CD-ROM), paper No. 2032.

MacGregor, J. G. and Bartlett, F. M. (2000). Reinforced Concrete: Mechanism and Design (Canadian Edition), First Edition. Prentice Hall Canada Inc., Scarborough, Ontario.

Meier, U., Deuring, M., Meier, H, and Schwengler, G. (1992). Strengthening of Structures with CFRP Laminates: Research and Applications in Switzerland. *1st International Conference on Advanced Composite Material in Bridges and Structures.* 243-251.

Paterson, J. and Mitchell, D. (2003). Seismic Retrofit of Shear Walls with Headed Bars and Carbon Fiber Wrap. *ASCE Journal of Structural Engineering.* **129:5**, 606-614.

Triantafillou, T. (1998). Shear Strengthening of Reinforced Concrete Beams Using Epoxy Bonded FRP Composites. *ACI Structural Journal.* **95:2**, 107-116.

Wong, P. S., and Vecchio, F. J. (2002). VecTor2 and FormWorks user's manual (Publication No. 2002-02). University of Toronto, Department of Civil Engineering.